Title: Formation of low molecular weight oligomers from chitin and chitosan stimulated by plasma-assisted processes

Author: <ce:author id="aut0005" author-id="S0144861717300267-b993974c688d670ae6b561ac4d95b96b"> T. Vasilieva<ce:author id="aut0010" author-id="S0144861717300267-3e1bc0c6624b10793fd7e34c9c45b0b9"> A. Sigarev<ce:author id="aut0015" author-id="S0144861717300267-500ac2e14adde52237df492de2dce7af"> D. Kosyakov<ce:author id="aut0020" author-id="S0144861717300267-de3dbb5cdb033cd9f0e8ca638739b683"> N. Ul'yanovskii<ce:author id="aut0025" author-id="S0144861717300267-b843aa29d2686deb88b0bede196d746f"> E. Anikeenko<ce:author id="aut0030" author-id="S0144861717300267-d8a836357b52819e8c24dcfb57c6356f"> D. Chuhchin<ce:author id="aut0035" author-id="S0144861717300267-d995fbbdd5eba9dc8eba94151de35f69"> A. Ladesov<ce:author id="aut0040" author-id="S0144861717300267-910dc43a2f63411e656449e4ef942ee1"> Aung Myat Hein<ce:author id="aut0045" author-id="S0144861717300267-d978754258ab2db1c5b0f4903dc502db"> V. Miasnikov

PII: S0144-8617(17)30026-7
DOI: http://dx.doi.org/doi:10.1016/j.carbpol.2017.01.026
Reference: CARP 11904

To appear in:

Received date: 23-8-2016
Revised date: 28-12-2016
Accepted date: 5-1-2017

Formation of low molecular weight oligomers from chitin and chitosan stimulated by plasma-assisted processes

T. Vasilieva[a, *], A. Sigarev[a], D. Kosyakov[b], N. Ul'yanovskii[b], E. Anikeenko[b], D. Chuhchin[b], A. Ladesov[b], Aung Myat Hein[c], V. Miasnikov[c]

[a]Department of General Chemistry, Moscow Institute of Physics and Technology, Institutsky per., 9, Dolgoprudny, Moscow region 141 700 Russia. Tel.: +7-916-550-27-40; fax: +7-495-408-67-98; e-mail: tmvasilieva@gmail.com
[b]Core Facility Center "Arktika", Northern (Arctic) Federal University, Severnaya Dvina Emb., 17, Arkhangelsk, Russia. e-mails: kosyakov@mail.ru; uluanovskii@mail.ru; dimatsch@lmail.ru; easorokina1992@mail.ru; lokoal13@gmail.com
[c]Aerospace Research Department, Moscow Institute of Physics and Technology, Institutsky per., 9, Dolgoprudny, Moscow region 141 700 Russia. e-mails: greatofaungmyathein52@gmail.com; vladimir.myasnikov@phystech.edu

[*] Corresponding author

Highlights

- Controllable chitin and chitosan destruction in Electron Beam Plasma was proved.
- Water-soluble chitooligosaccharides were formed abruptly at some treatment duration.
- 95% yield of chitooligosaccharides was attained by optimizing treatment conditions.
- Hazardous by-products and toxic wastes are not generated during treatment procedure.
- Plasmachemically produced chitooligosaccharides possessed antibacterial properties.

Abstract. The controlled degradation of solid powders of chitin and chitosan stimulated by electron-beam plasma (EBP) was experimentally studied. Crab shell chitin and chitosan were used as original substances. The non-equilibrium low temperature EBP was generated by injecting an electron beam into a gaseous medium. Chitooligosaccharides with M_w= 800-2000 Da and polydispersion 1.5-2.5 were formed due to the EBP-treatment of chitin and chitosan. The β-1,4 glycosidic bounds in original polymers degrade under the action of active oxygen species produced in the EBP. Low molecular weight products of chitosan inhibited the growth of various yeast-like and filamentous fungi at minimum inhibitory concentration 500 mcg/ml. By optimizing the treatment conditions and using special techniques of reaction volume formation the 95% yield of chitooligosaccharides was obtained after 2 min whereas the conventional chemical hydrolysis usually takes several days. The EBP-stimulated hydrolysis is promising for effective polysaccharides degradation and can be competitive with traditional technologies.

Keywords: electron-beam plasma, plasma-stimulated hydrolysis, chitin, chitosan, bioactive oligosaccharides

1. Introduction

Some natural renewable biopolymers such as chitin (linear heterocopolymer of β-1,4-linked 2-amino-2-deoxy-D-glucopyranose and 2-acet-amido-2-deoxy-D-glucopyranose units) and, its deacetylated derivative chitosan are very promising for technological and industrial applications, e.g. agriculture, pulp and paper subsector, microbiology, food processing, modern scientific fields like Extreme Biomimetics [Anitha et al., 2014; Bazhenov et al., 2015; Ehrlich et al., 2013; Szatkowski et al., 2015; Wysokowski et al., 2015] and especially in medicine, pharmacology and pharmaceutics [Dragostin et al., 2016; Laurienzo, 2010; Mekhail, Jahan, & Tabrizian, 2014; Ray, 2011; Ye et al., 2013; Zargar, Asghari, & Dashti, 2015]. The latter application is due to the unique biological properties namely high biocompatibility with living tissues, biodegrability, ability to the complexation, and low toxicity. In medicine and pharmaceutics water-soluble low molecular weight chitosans (LMWC) with weight average molecular mass (M_w) in the range of 5-10 kDa and chitooligosaccharides (COS, M_w less than 10 kDa) are usually required. These substances can be used as immune response-modulating or antibacterial agents, sorbents, radioprotectors, for the production of microcapsules and drug delivery systems, substrates and scaffolds for cell cultures [Liu, Zhang, Jin, Jiang, & Jia, 2013; Puras et al., 2013; Sharp, 2013; Silva-Dias et al., 2014].

To produce low molecular weight oligosaccharides several techniques, including chemical and enzymatic hydrolysis, and radiation treatment by γ-irradiation and high-energy ion and electron beams (with energies of several MeVs) have been suggested [Aranaz et al., 2009;

Goycoolea, Agullo, & Mato, 2004; Inthanon et al., 2012; Saranwong et al., 2012; Zargar, Asghari, & Dashti, 2015].

Simple and respectively low-cost chemical hydrolysis in concentrated acids or alkalis at high temperature is a conventional method. Toxic wastes and environment contamination are inherent in the chemical processing of polysaccharides. Because of chitin insolubility its hydrolysis is possible only under heterogenic conditions and chemical processes in liquids are usually used for deacetylated derivatives production. Often at the next stage the reacetylation of the formed LMWC has to be performed. In contrast, the enzymatic chitin hydrolysis results in the acetylated monoglucosamine formation but its yield is very low for practical applications [Aiba & Muraki, 1997; Goycoolea, Agullo, & Mato, 2004; Lin, Wang, Xue, & Ye, 2002; Roberts, 1992]. Both chemical and enzymatic methods of chitin and chitosan degradation are time consuming multi-stage procedures and usually take several hours [Scheel & Thiem, 1997; Zargar, Asghari, & Dashti, 2015].

The radiation treatment of chitosan is also complicated because of limited controllability of treatment conditions, high power consumption, and operation complexity of electron accelerators [Zhao & Mitomo, 2008, 2009; Yoshii, 2003] and γ-radiation isotope sources [Chmielewski, 2010; Pasanphan, Rimdusit, Choofong, Piroonpan, & Nilsuwankosit, 2010; Rashid, Rahman, Kabir, Shamsuddin, & Khan, 2012]. The molecular mass of produced LMWC decreased only 2-3 times with respect to the original polysaccharide while their polydispersion index increased [Kim, Choi, & Noh, 2008; Kim, Choi, Park, & Noh, 2008]. The radiation technologies are mostly applied for the treatment of high concentrated chitosan solutions and composite chitosan hydrogels production [Chmielewski, 2010; Pasanphan, Rimdusit, Choofong, Piroonpan, & Nilsuwankosit, 2010; Rashid, Rahman, Kabir, Shamsuddin, & Khan, 2012].

Thus, the development of effective techniques for quick and environment friendly polysaccharides degradation is the burning issue of the day. The plasmachemical technologies using non-equilibrium low temperature plasmas could be a promising alternative to the hydrolysis methods mentioned above. Chitosan modification and derivatization in gas discharge plasmas and chitosan destruction in liquid-phase plasma systems by a high frequency bipolar pulsed DC (direct current) discharge have been demonstrated in several studies [Ogino, Kral, Yamashita, & Nagatsu, 2008; Silva et al., 2008; Wu, Lee, Lin, Shaw, & Yang, 2010; Yin, Ren, & Wang, 2013; Zhang et al., 2012]. However the treated substrates were thin chitosan films or chitosan solutions and preliminary preparations were needed. Many factors can affect the treatment uniformity in discharge systems (such as possible instabilities of plasma reaction volume, complicated control of temperature distribution over the samples surface) and therefore the repeatability of the obtained results.

The present paper considers a novel approach to the production of water-soluble low molecular weight oligosaccharides based on the application of the Electron Beam Plasma (EBP).

The EBP is generated by injecting an electron beam (EB) into a gaseous medium. Under typical conditions of the EBP generation (medium pressure $1 < P_m < 10$ kPa and moderate EB power $N_b < 1$ kW) plasma is strongly non-equilibrium and cold. With respect to gas discharge plasmas the EBP has the following advantages [Vasiliev, 2001; Vasiliev, Win, & Pobol, 2014; Vasiliev & Vasilieva, 2016; Walton, et al., 2004]:

- The EB can be injected into any gases, vapors and gas-vapor mixtures.
- The EBP bulk does not contract even at very high gas pressures (P_m ~10 kPa and higher).
- Solid powders injected into the gas do not prevent the EBP generation.
- Very high concentrations of chemically active particles can be obtained even at low (~ 300 K) temperatures.
- The process of the EBP-treatment is absolutely controllable and the treatment results are replicable.

The aims of the present study were as follows:

- To experimentally prove the possibility of chitin and chitosan powders destruction and water-soluble COS formation as a result of plasmachemical processing in the EBP.
- To characterize the structure, molecular mass, and bioactivity of the produced COS.
- To obtain higher yield of the water-soluble LMWC and COS by optimizing the EBP-treatment conditions.

2. Materials and methods

2.1. Materials

Original substances for the further EBP-treatment were crab shell high molecular weight chitin (viscosity-average molecular weight, M_v = 1000 kDa) and chitosans (M_v = 200-500 kDa or *z*-average mass M_z= 12.0-25.0 kDa) with the deacetylation degree 95% and polydispersity index 1.5-2.5. Characteristic particle size of polysaccharides powders was ~ 100 μm. The polysaccharides were obtained from Bioprogress Co., Russia. All substances were not water-soluble.

Water originally absorbed by polysaccharide powder can significantly affect the treatment results. To eliminate this effect the powders to be treated were preliminary dried in vacuum 10^{-3} Pa overnight to decrease the content of water content associated with polysaccharides molecules.

2.2. Characterization of the EBP-treated polysaccharides

2.2.1. Solubility measurements

100±0.1 mg of the preliminary dried sample (m_s) were placed into a tube and 1.5 ml of distilled water were added to the sample. The resulting mixture was incubated for 24 h at room temperature under periodic mixing. After the incubation the mixture was centrifuged for 5 min and 1 ml of centrifugate was taken and dried. The mass of the dry residue (m_{dr}) was measured with an accuracy ±0.1 mg. The sample solubility was calculated as the (m_{dr}/ m_s)×100% ratio.

2.2.2. Determination of molecular weight

The molecular masses (weight-average M_w, number-average M_n, and *z*-average mass M_z) of the EBP-treatment products were determined by the size exclusion chromatography on a LC-20 Prominence HPLC system (Shimadzu, Japan) equipped with refractometric detector RID-10A. The chromatographic column was Polargel-M 300×7.5 mm (Agilent, USA). Other analysis conditions were as follows: the mobile phase – 0.1 M NaCl aqueous solution containing 0.01% trifluoroacetic acid; the flow rate – 1.0 ml/min; temperature - 40°C; volume of the injected sample – 20 μl; duration of the analysis – 20 min. The concentration of chitosan solutions was 1.0 mg/ml. Pullulans (Agilent, USA) with M_w= 340-45500 Da were used as standard samples (concentration of the solutions 1.0 mg/ml) for mass scale calibration. The WinGPC software (PSS, Germany) was applied to process the measurement data.

2.2.3. Matrix-assisted laser desorption/ionization mass spectrometry (MALDI)

MALDI mass spectra were recorded in the positive linear and reflectron modes by an Axima Performance mass spectrometer (Shimadzu-Biotech, Manchester, UK) equipped with a time-of-flight mass analyzer (TOF/TOF). We used a nitrogen UV laser (λ =337 nm) with pulse duration of 3 ns and energy of 130 μJ and working frequency of 50 Hz. The spectrum was obtained by accumulating the data of 200 laser shots (100 profiles each of 2 shots), collected from different points of the target. In all experiments the laser power exceeded the ionization threshold value of the analyzed samples by 10–20%. The mass scale was calibrated by means of the ProteoMass peptides kit (Sigma, Germany). The mass spectra were recorded in two ranges of m/z, 1000–20000 and 200–1000. The delayed pulse extraction of ions was optimized at m/z 2300 and 700 correspondingly. The mass spectrometer operation as well as the data acquisition and processing were controlled by the Launchpad software, version 2.9.

Sample solutions were prepared by dissolving 1 mg of polysaccharide in 1 mL of 0.1% aqueous solution of trifluoroacetic acid (TFA). 2.5-Dihydroxybenzoic acid (DHB) was used as a matrix and sodium chloride as a cationizing agent. 10 mg of DHB were dissolved in 1 mL of water-methanol mixture (1:1), containing 0.1% of TFA and 0.1% NaCl. Equal volumes (0.5 μL) of sample and matrix solutions were mixed on stainless steel MALDI target and dried in air at room temperature.

2.2.4. IR-spectroscopy

Solutions from the original and the EBP-treated chitosans were prepared by dissolving them in 1% acetic acid and the distilled water respectively. The solutions were casted and dried at 37°C to form thin films of 8.0±1.5 μm thick. The obtained films were then analyzed by the Fourier transform infrared (FT-IR) spectroscopy. In particular, the film thickness was estimated by analyzing of a baseline modulation period in a transmittance spectrum of the chitosan film.

IR spectral measurements in a wavenumber (ν) range 500-5000 cm^{-1} with a resolution of 4 cm^{-1} were carried out by a FT-IR spectrometer Perkin-Elmer Spectrum 100 (Perkin-Elmer, USA). A transmittance spectrum of the studied film, $T(\nu)$, was measured at normal incidence of IR radiation to the film surface as a ratio $T(\nu) = T_1(\nu)/T_0(\nu)$, where $T_0(\nu)$ and $T_1(\nu)$ are the registered transmission spectra of the spectrometer channel for an empty sample holder and for a sample holder with the film, respectively. The averaging of 16 scans was used to get good signal-to-noise ratio. The transmittance spectrum was converted to obtain the absorbance spectrum of the film, $A(\nu)$, through the equation $A(\nu) = -\log_{10}(T_1(\nu)/T_0(\nu))$.

2.2.5. Biological activity of the EBP-produced COS

The inhibition of the bacteria growth *in vitro* was measured to quantitatively characterize the bioactivity of the COS obtained by the EBP-treatment, gram-positive (*Staphylococcus aureus* ATCC 6538 P), gram-negative (*Escherichia coli* ATCC 25922) microorganisms, yeast-like (*Candida albicans* ATCC 855-653, *Candida scotti*, and *Rhodotorula rubra*) and filamentous (*Penicillium tardum, Penicillium chrizogenum, Penicillium crustozum, Aspergillus flavus, Aspergillus fumigatus, Phoma betae, Cladosporium herbarum, Mucor pusillus*, and *Trichoderma harzianum*) fungi being tested in these experiments.

S. aureus is commonly associated with food products as a result of human handling. *E.coli* was chosen because it is responsible for more infections than all other genera combined. Bacteria were supplied by "Central Research Institute of Epidemiology" of the Federal Service on Customers' Rights Protection and Human Well-being Surveillance (Moscow, Russia). All procedures were carried out in accordance with rules of State Pharmacopoeia of Russian Federation.

The EBP-produced COS were dissolved in deionized water at initial concentration 2000 μg/ml and then1000-125 μg/ml solutions were prepared using serial two-folds dilution method. Four replications for each COS concentration were made. All solutions were sterilized before being added to bacteria cultures.

The cells in the stationary phase of growth were centrifuged at 1300 × g for 20 min at 5 °C, and the pellets were resuspended in PBS (pH = 6.0) or beef-extract broth (pH = 7.2) to give viable bacteria number of 5×10^7 CFU/ml (resting bacteria) or 5×10^6 CFU/ml (replicating bacteria) in the final sample respectively (CFU - colony forming unit). Then the 0.1 ml of the

COS solutions or deionized water were added to tested and reference microorganism samples, respectively. Three replicate experiments were performed for both *S. aureus* and *E.coli* in their resting and replicating forms. The samples were incubated for 48 h at 37 °C at constant pH with shaking and then the microorganisms were firmly seeded over the Mueller-Hinton Agar (Lab M, UK) plates. The inhibitory effect of the EBP-produced COS was estimated visually after 72 h with respect to reference sample.

Fungicide activity of the EBP-produced COS was characterized in buffer system (pH = 6.5) containing the mixture of morpholineethanesulfonic, N-(2-acetamido)-2-aminoethanesulfonic, and 2-[Tris(hydroxymethyl)methylamino]-1-ethanesulfonic acids. Minimal inhibitory (MIC) and Minimal bactericidal (MBC) concentrations of COS were determined. Three replicates for each tested microorganism were used.

3. The EBP-treatment procedure

Controllable EBP-stimulated hydrolysis of polysaccharides was performed in a special Electron Beam Plasmachemical Reactor (EBPR). The EBPR, its operation modes and optimization of the biomaterial treatment regimes were described in detail in [Vasilieva, 2010].

Fig. 1 illustrates the design and operation of the EBPR. The focused EB 3 generated by the electron-beam gun 1 that is located in the high vacuum chamber 2 is injected into the working chamber 5 filled with the plasma-generating gas through the injection window 4. In passing through the gas the EB is scattered in elastic collisions and the energy of fast electrons gradually diminishes in various inelastic interactions with the medium (ionization, excitation, dissociation). As a result, the EBP cloud 10 is generated, all plasma parameters being functions of *x*, *y*, and *z* coordinates (*z* is the axis of the EB injection).

The electromagnetic scanning system 12 placed inside the working chamber near the injection window is able to deflect the injected EB axis in *x* and *y* directions and, therefore, to control the spatial distribution of the plasma particles over the plasma bulk. The working chamber is preliminary evacuated to pressure ~ 1 Pa and then filled with the plasma generating media.

In the preliminary experiments [Vasilieva, Lopatin, & Varlamov, 2016] the polysaccharide powder partially filled the glass container over the thin plate made of piezoelectric ceramics placed at the container bottom. Being fed with AC-voltage the plate vibrates, throws up the powder particles and forms the mixing layer of the treated material inside the container (Fig 2a). Our previous experiments showed that only 500 mg (or less) of polysaccharides powders can be effectively and uniformly modified in the reactor of this type.

To produce low molecular weight oligosaccharides in amounts sufficient for practical uses (up to tens or even a hundred of grams) a special mixing device was designed (Fig. 1). The device composed of cylindrical quartz vessel 10 with internal partitions 9 was equipped with a stepper motor rotating the vessel in various modes (continuous, intermittent, reverse, etc.). The device was placed inside the EBPR working chamber filled with the plasma generating gas at required pressure; as a result the aerosol reaction zone 7 is formed inside the chamber. Fig. 2b presents the photo of the polysaccharides powders EBP-treatment in the mixing device.

For the new reactor optimal treatment conditions (from the point of view of molecular mass and chemical structure of the COS and the treatment efficiency) were found. The optimized conditions were as follows:

- The plasma generating media – chemically pure oxygen and oxygen-water vapor mixtures with partial pressures ratio 2:1. The oxygen-water vapor plasma generating media was obtained by mixing chemically pure oxygen (Sigma-Aldrich, Germany) with vapor of bidistilled water produced by water evaporator 13 placed inside the EBPR working chamber. The composition of media was monitored throughout the entire treatment process by IR- and mass-spectrometers (AvaSpec-NIR256-1.7 (Avantes, the Netherlands) and HALO 201-RC (Hiden Analytical, UK) respectively). The oxygen containing media were used for our experiments because they were found to be the most effective for COS production compared with to other studied gases (nitrogen, ammonia, and noble gases) [Vasilieva, Lopatin, & Varlamov, 2016].
- The pressure of the plasma generating gas (P_m) was 133-670 Pa.
- The distance between the injection window and sample surface – 250 mm.
- The EB scanning mode – concentric circles with maximal diameter 130 mm. The optimal scanning mode was chosen in accordance with our previous studies [Vasilieva, & Lysenko, 2007].
- Treatment time τ was varied from 1 to 20 min.
- To prevent thermal destruction of the material all samples were processed at material temperature T_s = 40 °C. The sample temperature was monitored during the treatment by non-contact IR-pyrometer Optris LS (Optris GmbH, Germany) or by a miniature thermo-sensor inserted into the reaction zone. The temperature control was carried out by selecting the EB current I_b ($1 < I_b < 100$ mA).

4. Results and discussion

4.1. Characterization of structure and molecular weight of the COS produced by the EBP-stimulated degradation

The original chitin and chitosan were not water-soluble while the EBP-treatment increased their solubility in water due to the COS formation. Molecular masses of the COS produced by the EBP-stimulated degradation were characterized by exclusion chromatography. The molecular weight of chitosans markedly decreased (to ~1 kDa or less) after the first minute of the EBP-treatment, the molecular masses of the formed products did not depend on the initial molecular weight of original biopolymers.

In Table 1 the dependence of the COS molecular mass/time for the chitosan with initial M_z = 13.3 kDa treated in the oxygen EBP is given. The exclusion chromatography of the EBP-treated chitosans treated in the EBP of oxygen or water vapor for τ = 1-4 min revealed the formation of a number of the COS with M_w ~ 600-800 Da with polydispersity 1.1-1.0, that corresponds to the formation of fragments with degradation degree varied from dimeres to trimers. After τ more than 10 min small fragments with M_w ~190 Da were produced and further treatment did not result in additional decrease of the COS molecular weight.

The IR transmittance $T(\nu)$ spectra of the chitosan film prepared from original (M_z= 13.3 kDa) in the middle IR-range of ν from 500 cm^{-1} to 5000 cm^{-1} were measured before and after treatment in the EBP of oxygen gas for 5 min. The overall spectra and the fragments of the respective absorbance $A(\nu)$ spectra in the range 800-2000 cm^{-1} are shown in Figures 3 and 4, respectively. Spectral positions of selective absorption peaks (transmittance minima) and assignments of the corresponding characteristic absorption bands are given in Table 2. Identification of the absorption bands was carried out in accordance with [Balau, Lisa, Popa, Tura, & Melnig, 2004; Ehrlich et al., 2007; Kumirska et al., 2010; Ma, Wang, Wu, He, & Wu, 2014; Ma, Wang, Zhao, & Tian, 2012]. A weak periodic modulation of the baselines in the obtained IR spectra is caused by interference of the IR radiation in chitosan films. A general level of the baseline is related to nonselective reflection and scattering of the IR radiation from the film.

Fig. 3 shows that the strong wide bands with absorption peaks at 3400-3470, 3365, 3300, 2920 and 2850 cm^{-1} (Table 2) in the range 3700-2700 cm^{-1} and the bands at 1380, 1320 and 1260 (Table 2) in the range 1500-1200 cm^{-1} exhibit almost no significant differences in the transmittance spectra of either original or treated chitosan films. However, Fig. 3 and 4 show some differences in the above spectra within the wavenumber range 1500-2000 cm^{-1}. It is important to note that in the spectra of the treated chitosan film (red curves in Fig. 3 and Fig. 4)

the weak band at 1735 cm^{-1} corresponding to the stretching vibrations of C=O groups in carboxyl groups (–COOH) is observed. Note that this band was not observed in the spectrum of the original chitosan film. A comparison of the intensities of the absorption bands in the range 1700-1500 cm^{-1} (Fig. 4) shows, that the peak intensity for the band at 1592 cm^{-1} (corresponding to deformation vibrations of NH_2 groups) is almost the same for both spectra. However, the selective peak intensity (the difference between the absorbance values at the maximum and at the baseline level) for the band at 1650 cm^{-1} (corresponding to C=O stretching vibrations of Amide I groups) in the spectrum for the treated chitosan film is approximately 20% higher than that in the absorbance spectrum of the original film. Also there is small decrease in the integral intensity of the bands at 1422, 1155 and 896 cm^{-1} in the range 1250-500 cm^{-1} (Table 2). Note, the bands at 1155 and 896 cm^{-1} correspond to β-1,4-glycosidic bonds [Ehrlich et al., 2007; Kumirska et al., 2010; Ma, Wang, Zhao, & Tian, 2012; Ma, Wang, Wu, He, & Wu, 2014]. So the analysis of the IR absorption spectra of the original and treated chitosan films showed that the EBP-treatment resulted in some increase of oxygen-containing carbonyl C=O and carboxyl –COOH groups and some destruction of the β-1,4-glycosidic bonds.

4.2. The time-dependence of the water-soluble COS production

The maximum yield S_{max} (up to 90-95%) of the water-soluble COS could be obtained by optimizing the conditions of the EBP-stimulated hydrolysis (for example the treatment duration or the composition and the pressure P_m of the plasma generating media).The variation of the water-soluble COS yield as a function of the treatment time $S(\tau)$ is shown in Fig. 4. At first the dependence $S(\tau)$ increases smoothly, then – steeply close to $\tau_0 = 2$ min after which the yield of the water-soluble products does not change. When the treatment duration exceeded 10 min the COS condensation occurred, which resulted in the high molecular products formation due to the reaction between aldehyde and amino groups contained in the chitosan chemical structure and the loss of solubility (Fig. 5).

The COS formed due to the EBP-stimulated hydrolysis for τ=1-20 min were also characterized by MALDI mass spectrometry. Two groups of the MALDY lines in ranges *m/z* 200–1000 and 1500–5000 were detected in the MALDY spectra of original chitosan, the intensity of the first group being the highest (Fig. 6). The intervals between lines were found to be equal to 161 Da that corresponds to the molecular mass of one structure unit in chitosan macromolecule. The additional pattern of the MALDY lines with the 42 Da shift to the high molecular mass range (C_2H_2O) indicates the presence of acetylated derivatives in the original chitosan sample.

The plasmachemical chitosan hydrolysis changed the MALDY spectra, the most significant differences were observed in the high molecular mass range (Fig. 6b). Almost total loss of the acetyl groups occurred after 1 min of the EBP-treatment. The prolongation of the treatment time up to 8 min resulted in the formation of low molecular weight fragments. The MALDY lines in the *m/z* range higher than 1000 did not reveal in the spectra after 20 min of EBP- hydrolysis due to the intensive chitosan macromolecules destruction.

The shift to the lower *m/z* values was also found in the MALDY spectra recorded within low molecular weight *m/z* range (≥1000) (Fig. 6a). After 10 min of the EBP-treatment a number of intensive lines were found in *m/z* range 300-500, which confirms the formation of the trimeric and dimeric COS with various functional composition. The most significant line with *m/z* 345 corresponds to the dehydrated dimeric ion $[M\text{-}H_2O+Na]^+$. The EBP-stimulated hydrolysis for τ = 12-20 min resulted in the formation of large amounts of low molecular weight products and the MALDY lines are revealed almost at any integer *m/z*.

The rise of the basic line and the diffusive signals in *m/z* range 5000–20000 detected in the MALDY spectra of chitosan after the EBP-treatment for τ = 12 and 20 min are of considerable interest. Such observations support the fact that the $S(\tau)$ dependence described above could be due to the secondary EBP-stimulated polymerization of low molecular weight COS intermediates.

The similar $S(\tau)$ relations were found for chitin. For example τ_0 for the chitin destruction in the oxygen EBP (P_m = 133 Pa) using the mixing device was 10 min. It should be noted that the chemical modification of chitin oligomers produced in the EBP is negligible. The reversed-phase chromatography performed in our preliminary studies revealed that the elution time of the chitin oligomers produced in the EBP is the same as that of the control chitin oligomers markers [Vasilieva, Lopatin, & Varlamov, 2016].

4.3. The degradation mechanisms of polysaccharides in EBP

The EBP composition is complex: generally it contains chemically active molecules, atoms, radicals and ions in stable and excited states, high energy electrons of the primary beam and secondary plasma electrons that can be also be highly energetic. Bremsstrahlung and UV-irradiation, generated in EBP can affect the polysaccharides structure as well. In our previous studies it was proved that all these factors are responsible for the degradation of the original biopolymer but the plasmachemical processes predominate [Vasilieva, & Lysenko, 2007; Vasil'eva, & Chukhchin, 2008]. The radiation and thermal damage of the polysaccharides due to

high energy electrons was minimized by proper selection of plasma generating gas pressure and the EB scanning mode.

In plasmas of oxygen and water vapor active oxygen particles (O, $O^{\bullet}$, singlet oxygen) formed in plasmachemical reactions and products of the water plasmolisys (e.g. $OH^{\bullet}$) seem to be the most important. These chemically active particles initiate radical chain reactions in the biopolymers that cause destruction of β-1,4-glycosidic bonds and decrease the polysaccharides molecular weight. The radicals formation in the EBP-treated polysaccharides was proved by means of the electron paramagnetic resonance spectroscopy. The possible degradation mechanisms were considered in [Chang, Tai, & Cheng, 2001] and our previous papers [Vasilieva, Lopatin, Varlamov, & Aung Tun Win, 2015; Vasilieva, Lopatin, & Varlamov, 2016].

The M_w of products obtained after chitin and chitosan EBP-treatment for 1-20 min were approximately equal. It means that mechanisms of the EBP-stimulated depolymerization for both chitin and chitosan are likely to be the same. The destruction of β-1,4-glycosidic bonds by oxygen containing particles in oxygen EBP [Vasiliev, 2001; Vasiliev, & Vasilieva, 2016] that has been proved for cellulose confirms this conclusion.

Under the treatment conditions the temperature of the plasma generating media T_g did not exceed 40 °C (i.e. the EBP was really low temperature or cold). Since powder particles temperature is approximately equal to T_g possible thermal destruction of the polysaccharides was absolutely excluded.

4.4. Characterization of biological activity of the COS produced by the EBP-stimulated degradation

Several studies carried out on *Bacillus cereus*, *E. coli*, *S. aureus*, *Pseudomonas aeruginosa*, *Salmonella enterica*, *B. subtilis*, *Listeria monocytogenes*, *Klebsiella pneumoniae*, and some other species, proved that the biological activity of chitosan significantly depends on its molecular weight. Chitosans with lower molecular mass demonstrated the greater reducing of microorganism growth and multiplication [Benhabiles et al., 2012; Fernandes et al., 2010; Jing et al., 2007; Silva-Dias et al., 2014; Tikhonov et al., 2006 ; Tsai, Zhang, & Shieh, 2004; Wang et al., 2007]. The LMWC size and conformation appear to be very important to control their effectiveness. The mobility, attraction and ionic interaction of small chains are higher and stronger than of long ones facilitating the adoption of extended conformation and strong binding to the bacterial membranes [Goy, Britto, & Assis, 2009; Kumar, Varadaraj, Gowda, & Tharanathan, 2005].

Therefore the inhibition of the microorganism growth *in vitro* was studied to characterize the bioactivity of the COS formed in the EBP. The COS produced by the chitosan (M_v=500 kDa) EBP-treatment in water vapor at concentration 1000 μg/ml were found to completely suppress

the multiplication of both *S. aureus* and *E. coli* in replicating and resting forms. Some results for replicating bacteria are shown in Table 3. The products obtained by the treatment of chitosan in the oxygen EBP for 5 min inhibited the growth of filamentous fungi *P. tardum*, *P. chrizogenum*, *A. flavus*, *P. betae*, and *C. herbarum* at final concentration (MBC) 500 μg/ml up to 99,9% while the rest studied filamentous fungi decreased the spore formation. The most sensitive yeast-like fungi were *C. scotti* and *R. rubra* (with MIC 500 μg/ml and 250 μg/ml, respectively). We suppose that the antibacterial activity of the EBP-produced low molecular weight chitooligosaccharides results from their interaction with the cell walls of microorganisms. This mechanism was considered in detail in [Wang et al., 2007].

5. Conclusions

1. The possibility of the EBP-stimulated degradation of native chitin and chitosan and formation of the water-soluble COS was proved experimentally.
2. The 90-95% yield of the water-soluble COS was attained by optimizing the EBP-treatment procedure. The high yields of low molecular weight water soluble products are obtained at treatment time ~ 2 min whereas the traditional chemical chitosan hydrolysis usually takes several days. The hazardous by-products and toxic wastes are not generated during the EBP-treatment. The active oxygen species produced in plasmachemical reactions and the products of water plasmolisys are responsible for the COS formation.
3. The low molecular water-soluble forms of the chitosan obtained by its treatment in the EBP of oxygen and water vapor were found to inhibit the growth of *S. aureus, E. coli,* yeast-like and filamentous fungi.

Thus, our experiments have demonstrated that the EBP can be applied for the effective and controllable destruction of chitin and chitosan. The technique involved seems to be competitive with technologies conventionally used in the chemical and biotechnological industries. The water-soluble COS produced by the EBP-treatment of polysaccharides have new biological activities (for instance, the effective antimicrobial or fungicidal properties) and are likely to be promising agents for pharmaceutical, medical, and agricultural applications.

Acknowledgements

This research was performed using the instrumentation of Core Facility Center “Arktika” of Northern (Arctic) Federal University under financial support of the Ministry of Education and Science of Russian Federation.

The work is supported by RFBR (grant 15-08-05724_a).

References

Anitha, A., Sowmya, P.T., Kumar, S., Deepthi, S., Chennazhi, K.P., Ehrlich, H., Tsurkan, M., & Jayakumar, R. (2014). Chitin and chitosan in selected biomedical applications. *Progress in Polymer Science, 39*, 1644-1667.

Aranaz, I., Mengibar, M. M., Harris R., Panos, I., Miralles B., Acosta, N., Galed, G., & Heras, A. (2009). Functional characterization of chitin and chitosan. *Current Chemical Biology*, *3*, 203-230.

Balau, L., Lisa, G., Popa, M. I., Tura, V. & Melnig, V. (2004). Physico-chemical properties of chitosan films. *Central European Journal of Chemistry*, *2*, 638-647.

Bazhenov, V. V., Wysokowski, M., Petrenko, I., Stawski, D., Sapozhnikov, P., Born, R., Stelling, A. L., Kaiser, S., & Jesionowski, T. (2015). Preparation of monolithic silica-chitin composite under extreme biomimetic conditions. *International Journal of Biological Macromolecules, 76*, 33-38.

Benhabiles, M. S., Salah, R., Lounici, H., Drouiche, N., Goosen, M. F. A., & Mameri, N. (2012). Antibacterial activity of chitin, chitosan and its oligomers prepared from shrimp shell waste. *Food Hydrocolloids*, *29*, 48-56.

Chang, K. L. B., Tai, M. C., & Cheng, F. H. (2001). Kinetics and products of the degradation of chitosan by hydrogen peroxide. *Journal of Agricultural and Food Chemistry*, *49***,** 4845-4851.

Chmielewski, A. G. (2010). Chitosan and radiation chemistry. *Radiation Physics and Chemistry*, *79*, 272-275.

Dragostin, O. M., Samal, S. K., Dash, M., Lupascu, F., Panzariu, A., Tuchilus, C., Ghetu, N., Danciu, M., Dubruel, P., Pieptu, D., Vasile, C., Tatia, R., & Profire, L. (2016). New antimicrobial chitosan derivatives for wound dressing applications. *Carbohydrate Polymers*, *141*, 28-40.

Ehrlich, H., Maldonado, M., Spindler, K.-D., Eckert, C., Hanke, T., Born, R., Goebel, C., Simon, P., Heinemann, S., & Worch, H. (2007). First evidence of chitin as a component of the skeletal fibers of marine sponges. Part I. Verongidae (Demospongia: Porifera). *Journal of Experimental Zoology (Mol Dev Evol)*, *308B*, 347-356.

Ehrlich, H., Simon, P., Motylenko M., Wysokowski, M., Bazhenov B., Galli., R., Stelling, A. L., Stawski, D., Ilan, M., Stocker, H., Abendroth, B., Born, R., Jesionowski, T., Kurzydlowski, K. J., & Meyer D. C. (2013). Extreme biomimetics: formation of zirconium dioxide nanophase using chitinous scaffolds under hydrothermal conditions. *Journal of Materials Chemistry B, 1*, 5092-5099.

Fernandes, J. C., Tavaria, F. K., Fonseca, S. C., Ramos, O. S., Pintado, M. E., & Malcata, F. X. (2010). In vitro screening for anti-microbal activity of chitosans and chitooligosaccarides, aiming

at potential uses in functional textiles. *Journal of Microbiology and Biotechnology*, *20*, 311-318.

Goy, R. C., de Britto, D., & Assis, O. B. G. (2009). A review of the antimicrobial activity of chitosan. *Polímeros: Ciência e Tecnologia*, *19*, 241-247.

Goycoolea, F., Agullo E., & Mato, R. (2004). Fuentes y procesos de obtencion. In A. P. de Abram (Ed.), Quitina y quitosano: obtencion, caracterization y aplicaciones (pp. 105-156). Pontificia Universidad Catolica del Peru: Fondo Editoral.

Jing, Y. J., Hao, Y. J., Qu, H., Shan, Y., Li, D. S., & Du, R. Q. (2007). Studies on the antibacterial activities and mechanisms of chitosan obtained from cuticles of housefly larvae. *Acta Biologica Hungarica*, *58*, 75-86.

Kim M. S., Choi Y. J., & Noh I. (2008). Control of chitosan molecular weight with cyclotron ion beam irradiation. *Journal of Physics and Chemistry of Solids*, *69*, 1577-1580.

Kim M. S., Choi Y. J., Park H. S., & Noh I. (2008). Analysis of chitosan irradiated with high-energy cyclotron ion beams. *Journal of Physics and Chemistry of Solids*, *69*, 1569-1572.

Kumar, A. B. V., Varadaraj, M. C., Gowda, L. R., & Tharanathan, R. N. (2005). Characterization of chito-oligosaccharides prepared by chitosanolysis with the aid of papain and Pronase, and their bactericidal action against *Bacillus cereus* and *Escherichia coli*. *Biochemical Journal*, *391*, 167-175.

Kumirska, J., Czerwicka, M., Kaczynski, Z., Bychowska, A., Brzozowski, K., Thoming, J., & Stepnowski, P. (2010). Application of spectroscopic methods for structural analysis of chitin and chitosan. *Marine Drugs*, *8*, 567-1636.

Laurienzo, P. (2010). Marine polysaccharides in pharmaceutical applications: an overview. *Marine Drugs*, *8*, 2435-2465.

Lin H., Wang H., Xue C., & Ye, M. (2002). Preparation of chitosan oligomers by immobilized papain. *Enzyme and Microbial Technology*, *31*, 588-592.

Liu, Q. Y., Zhang, Z. H., Jin, X., Jiang, Y. R., & Jia, X. B. (2013). Enhanced dissolution and oral bioavailability of tanshinone IIA base by solid dispersion system with low-molecular-weight chitosan. *Journal of Pharmacy and Pharmacology*, *65*, 839-846.

Ma, F., Wang, Z., Zhao, H., & Tian, S. (2012). Plasma depolymerization of chitosan in the presence of hydrogen peroxide. *International Journal of Molecular Sciences*, *13*, 7788-7797.

Ma, Z., Wang, W., Wu, W., He, Y., & Wu, T. (2014). Oxidative degradation of chitosan to the low molecular water-soluble chitosan over peroxotungstate as chemical scissors. *PLOS ONE/www.plosone.org*, *9*, 1-7.

Mekhail, M, Jahan, & K, Tabrizian, M. (2014). Genipin-crosslinked chitosan/poly-L-lysine gels promote fibroblast adhesion and proliferation. *Carbohydrate Polymers*, *108*, 91-98.

Ogino, A., Kral, M., Yamashita, M., & Nagatsu, M. (2008). Effect of low-temperature surface-wave plasma treatment with various gases on surface modification of chitosan. *Applied Surface Science*, *255*, 2347-2352.

Pasanphan, W., Rimdusit, P., Choofong, S., Piroonpan, T., & Nilsuwankosit, S. (2010). Systematic fabrication of chitosan nanoparticle by gamma irradiation. *Radiation Physics and Chemistry*, *79*, 1095-1102.

Puras, G., Zarate, J., Aceves, M., Murua, A., Diaz, A. R., Aviles-Triguero, M., Fernandez, E., & Pedraz, J. L. (2013). Low molecular weight oligochitosans for non-viral retinal gene therapy. *European Journal of Pharmaceutics and Biopharmaceutics*, *83*, 131-140.

Rashid, T. U., Rahman, M. M., Kabir, S., Shamsuddin, S. M., & Khan, M. A. (2012). A new approach for the preparation of chitosan from γ-irradiation of prawn shell: effects of radiation on the characteristics of chitosan. *Polymer International*, *61*, 1302-1308.

Ray, S. D. (2011). Potential aspects of chitosan as pharmaceutical excipient. *Acta Poloniae Pharmaceutica*, *68*, 619-622.

Roberts G. A. F., (1992). *Chitin chemistry*. (1st ed.). London: The Macmillan Press Ltd., (Chapter 2).

Scheel, O., & Thiem, J. (1997) Cleavage of chitin by means of aqueous hydrochloric acid and isolation of chito-oligosaccarides. In R. A. A. Mizzarelli, & M. G. Peter (Eds.), *Chitin Handbook* (pp. 165-170). European Chitin Society: Atec, Grottammare.

Sharp, R. G. (2013). A review of the applications of chitin and its derivatives in agriculture to modify plant-microbial interactions and improve crop yields. *Agronomy*, *3*, 757-793.

Silva, S. S., Luna, S. M., Gomes, M. E., Benesch, J., Pashkuleva, I., Mano, J. F., & Reis, R. L. (2008). Plasma surface modification of chitosan membranes: characterization and preliminary cell response studies. *Macromolecular Bioscience*, *8*, 568-576.

Silva-Dias, A., Palmeira-de-Oliveira, A., Miranda, I. M., Branco, J., Cobrado, L., Monteiro-Soares, M., Queiroz, J. A., Pina-Vaz, C., & Rodrigues, A. G. (2014). Anti-biofilm activity of low-molecular weight chitosan hydrogel against *Candida* species. *Medical Microbiology and Immunology*, *203*, 25-33.

Szatkowski, T., Wysokowski, M., Lota, G., Peziak, D., Bazhenov, V. V., Nowaczyk, G., Walter, J., Molodtsov, S. L., Stocker, H., Himcinschi, C., Petrenko, I., Stelling, A. L., Jurga, S., Jesionowski, T., & Ehrlich, H. (2015). Novel nanostructured hematite-spongin composite developed using an extreme biomimetic approach. *RSC Advances*, *5*, 79031-79040.

Tikhonov, V. E., Stepnova, E. A., Babak, V. G., Yamskov, I. A., Palma-Guerrero, J., Jansson, H. B., Lopez-Llorca, L. V., Salinas, J., Gerasimenko, D. V., Avdienko, I. D., & Varlamov, V. P.

(2006). Bactericidal and antifungal activities of a low molecular weight chitosan and its *N*-/2(3)-(dodec-2-enyl)succinoyl/-derivatives. *Carbohydrate Polymers*, *64*, 66-72.

Tsai, G. J., Zhang, S. L., & Shieh, P. L. (2004). Antimicrobial activity of a low-molecular-weight chitosan obtained from cellulase digestion of chitosan. *Journal of Food Protection*, *67*, 396-398.

Vasiliev, M. (2001) Applications of electron-beam plasma in plasma chemistry. In V. E. Fortov (Ed.), Encyclopedia of low-temperature plasma. IX (pp. 436-445). Moscow: Nauka.

Vasiliev, M., Win, A. T., & Pobol, I. (2014). New applications of beam-plasma systems for the materials production. *International Journal of Nanotechnology*, *11*, 660-668.

Vasiliev, M., & Vasilieva, T. (2016). Materials production with beam plasmas. In J. L. Shohet (Ed.), Encyclopedia of plasma technology. Taylor & Francis Group: New York, USA.

Vasilieva, T. (2010). A beam-plasma source for protein modification technology. *IEEE Transactions on Plasma Sciences*, *38*, 1903-1907.

Vasilieva, T., Lopatin, S., & Varlamov V. (2016). Production of the low-molecular-weight chitin and chitosan forms in electron-beam plasma. *High Energy Chemistry*, 50, 150-154.

Vasilieva, T., Lopatin, S., Varlamov V., & Aung Tun Win. (2015). Controllable degradation of polysaccharides stimulated by electron-beam plasma. 22nd International Symposium on Plasma Chemistry. Antwerp, Belgium, paper P-II-11-11.

Vasilieva, T., & Lysenko, S. (2007). Factors responsible for biomaterials modification in the electron-beam plasma. *Journal of Physics: Conference Series*, *63*, 012033.

Vasil'eva, T. M., & Chukhchin, D. G. (2008). The effect of beam-plasma modification of fibrin-monomer on its biological properties. *High Energy Chemistry*, *42*, 404-407.

Walton, S. G., Muratore, C., Leonhardt, D., Fernsler, R. F., Blackwell, D. D., & Meger R. A. (2004). Electron-beam-generated plasmas for materials processing. *Surface Coatings and Technology*, *186*, 40-46.

Wang, Y., Zhou, P., Yu, J., Pan, X., Wang, P., Lan, W., & Tao, S. (2007). Antimicrobal effect of chitooligosaccarides produced by chitosanase from *Pseudomonas* CUY8. *Asia Pacific Journal of Clinical Nutrition*, 16, suppl. 1, 174-177.

Wu, Y. C., Lee, T. M., Lin, J. C., Shaw, S. Y., & Yang, C. Y. (2010). Argon-plasma-treated chitosan: surface characterization and initial attachment of osteoblasts. *Journal of Biomaterials Science Polymer Edition*, *21*, 563-579.

Wysokowski, M., Petrenko, I., Stelling, A. L., Stawski, D., Jesionowski, T., & Ehrlich, H. (2015). Chitin as a versatile template for extreme biomimetics. *Polymers*, *7*, 235-265.

Wysokowski, M., Petrenko, I., Motylenko, M., Langer, E., Bazhenov, V. V., Galli, R., Stelling, A. L., Kljajić, Z., Szatkowski, T., Kutsova, V. Z., Stawski, D., & Jesionowski, T. (2015). Renewable chitin from marine sponge as a thermostable biological template for hydrothermal

synthesis of hematite nanospheres using principles of extreme biomimetics. *Bioinspired Materials*, *1*, 12-22.

Wysokowski, M., Motylenko, M., Beyer, J., Makarova, A., Stoker, H., Walter, J., Galli, R., Kaiser, S., Vyalikh, D., Bazhenov, V. V., Petrenko, I., Stelling, A. L., Stawski, D., Kurzydlowski, K. J., Langer, E., Tsurkan, M. V., Jesionowski, T., Heitmann, J., Meyer, D. C., & Ehrlich, H. (2015). Extreme biomimetic approach for developing novel chitin-GeO2 nanocomposites with photoluminescent properties. *Nano Research*, 8, 2288-2301.

Ye, Y., Xu, Y., Liang, W., Leung, G. P., Cheung, K. H., Zheng, C., Chen, F., & Lam, J. K. (2013). DNA-loaded chitosan oligosaccharide nanoparticles with enhanced permeability across Calu-3 cells. *Journal of Drug Targeting*, *21*, 474-486.

Yin, S., Ren, L., & Wang, Y. (2013). Argon plasma-induced graft polymerization of PEGMA on chitosan membrane surface for cell adhesion improvement. *Plasma Science and Technology*, *15*, 1041-1046.

Yoshii F., Zhao L., Wach R.A., Nagasawa N., Mitomo H., Kume T. (2003). Hydrogels of polysaccharide derivatives crosslinked with irradiation at paste-like condition. *Nuclear Instruments and Methods in Physics Research Section B, 208,* 320-324.

Zargar, V., Asghari, M., & Dashti, A. (2015). A review on chitin and chitosan polymers: structure, chemistry, solubility, derivatives, and applications. *ChemBioEng Reviews*, *2*, 204-226.

Zhang, H. Y., Cleymand, F., Noel, C., Kahn, C. J., Linder, M., Dahoun, A., Henrion, G., & Arab-Tehrany, E. (2013). Effects of Ar-H2-N2 microwave plasma on chitosan and its nanoliposomes blend thin films designed for tissue engineering applications. *Carbohydrate Polymers*, *93*, 404-411.

Zhao, L. & Mitomo, H. (2008). Radiation effects on dihydroxypropyl-chitosan. *Polymer Degradation and Stability*, 93, 1607-1610.

Zhao, L. & Mitomo, H. (2009). Hydrogels of dihydroxypropyl chitosan crosslinked with irradiation at paste-like conditions. *Carbohydrate Polymers*, *76*, 314-319.

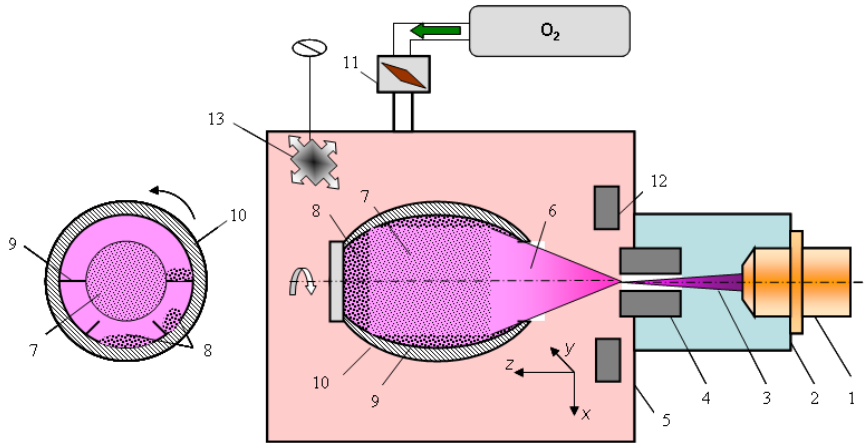

Fig. 1. The design of the plasmachemical reactor and the treatment procedure of polysaccharide powders.

1 – electron beam gun; 2 – high vacuum chamber; 3 – EB; 4 – injection window; 5 – working chamber; 6 – EBP cloud; 7 – aerosol reaction zone; 8 – polysaccharide powder to be treated; 9 – internal partitions; 10 – cylindrical quartz vessel; 11 – gas feeder; 12 – scanning system; 13 – water evaporator.

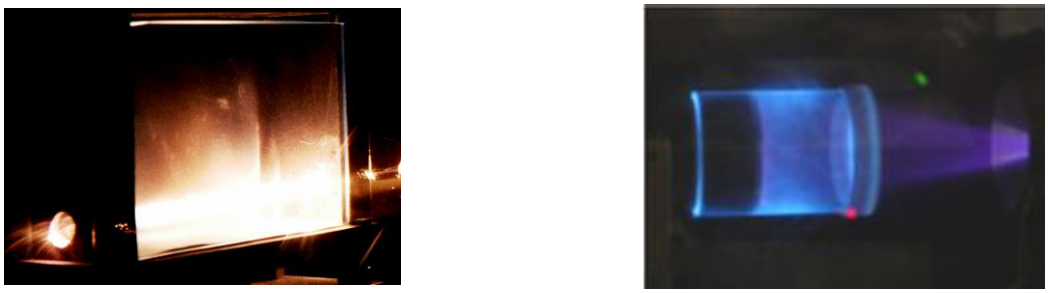

a) b)

Fig. 2. The mixing layer of polysaccharide powders in glass container (a), and the EBP-treatment of polysaccharide powders in rotating mixer (b).

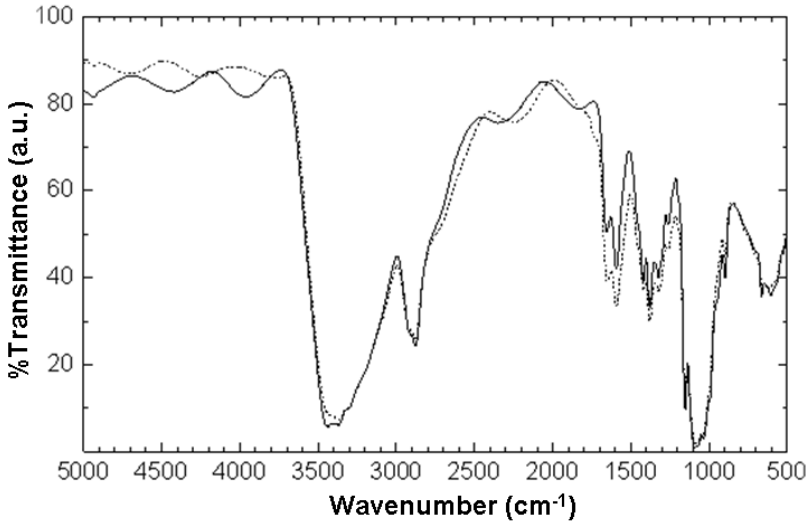

Fig. 3. The transmittance spectra in the wavenumber range 500-5000 cm^{-1} for a chitosan film ~8 μm thick before (solid curve) and after (dashed curve) the EBP-treatment in oxygen media.

‘

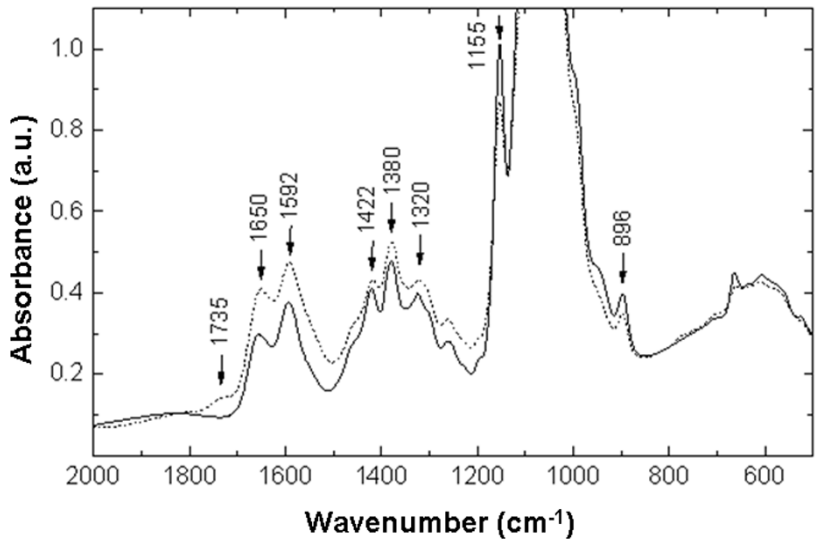

Fig. 4. Fragments of the absorbance spectra of the chitosan film ~8 μm thick before (solid curve) and after (dashed curve) the EBP-treatment in oxygen media in the range 500-2000 cm^{-1}.

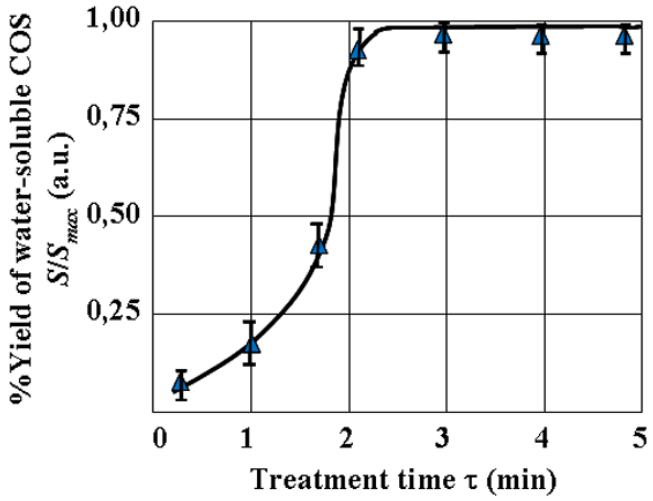

Fig. 5. The yield of the water-soluble LMWC (S/S_{max}) from the chitosan treated by the oxygen EBP as a function of the treatment time (τ).

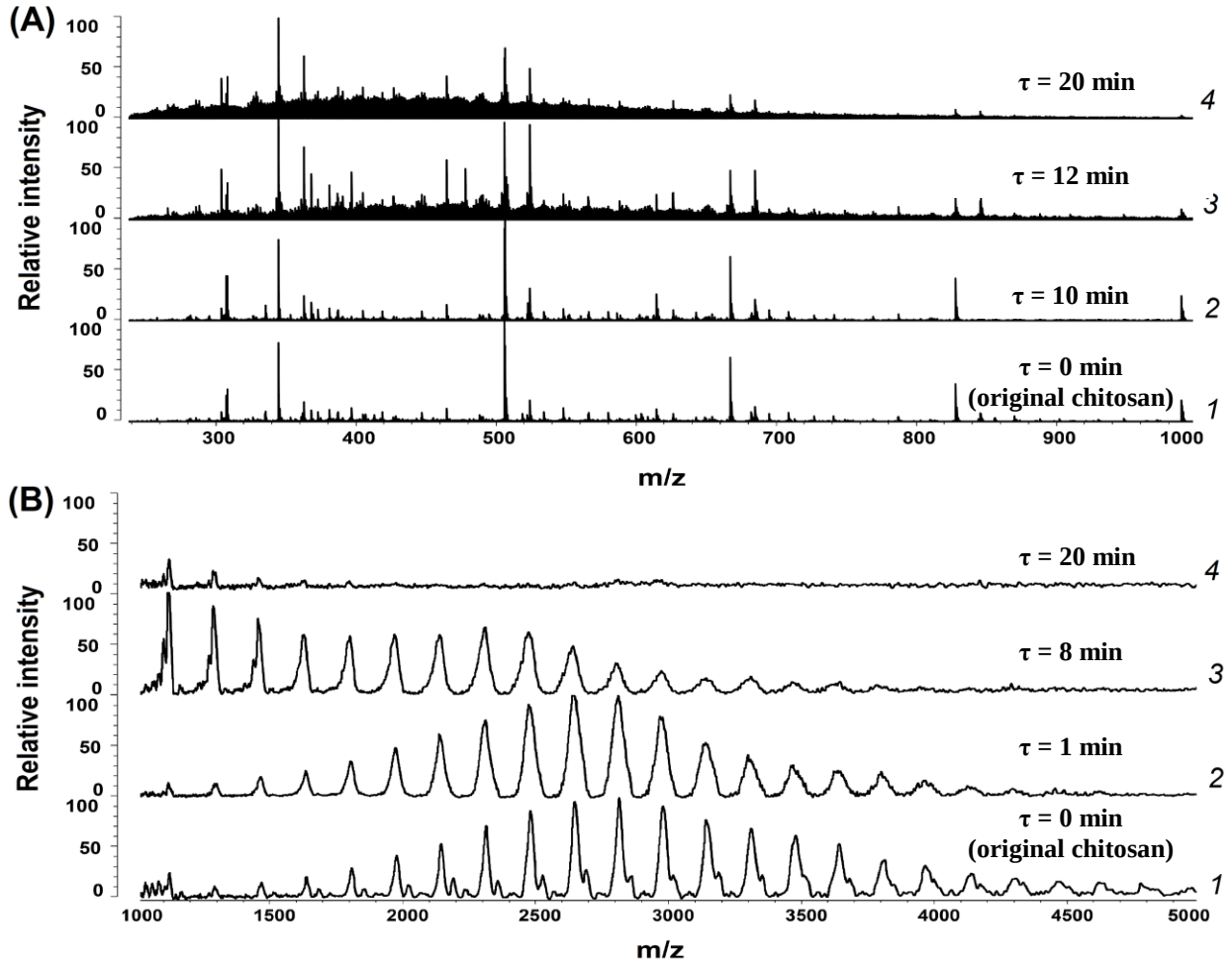

Fig. 6. The MALDI spectra recorded within the *m/z* ranges ≥1000 (a) and 1000-5000 (b) of the original and EBP-treated chitosan.

1 – original chitosan; 2, 3, and 4 – chitosan treated in the oxygen EBP, the duration of the EBP-treatment is given for the corresponding spectra

Table 1

Molecular weight of the COS formed due to the treatment of original chitosan (M_z = 13.3 kDa) in the oxygen EBP.

Treatment time (min)	M_n	M_w (Da)	M_z (Da)	Polydispersity index (M_w/M_n)
1	599	686	785	1.14
2	587	625	669	1.06
4	543	560	578	1.03
8	524	531	539	1.01
20	178	193	211	1.08

Table 2

Identification of the absorption bands in IR spectra of chitosan films made on the basis of [Balau, Lisa, Popa, Tura, & Melnig, 2004; Ehrlich et al., 2007; Kumirska et al., 2010; Ma, Wang, Zhao, & Tian, 2012; Ma, Wang, Wu, He, & Wu, 2014].

Absorption peak (cm^{-1})	Type of vibrations
3400-3470	stretching of OH groups
~3365	asymmetrical stretching of NH_2 groups
~3300	symmetrical stretching of NH_2 groups
2920	asymmetrical stretching of CH_2 groups
2850	symmetrical stretching of CH_2 groups
1735	C=O stretching of carboxyl groups (–COOH)
1650	C=O stretching of Amide I groups
1592	deformations of NH_2 (Amide II)
1422	deformations of CH_2 groups
1380	deformations of CH_2 groups
1320	deformations of CH_2 groups
1260	wagging of CH_2 groups
1160-880	vibrations of C-O-C groups, wagging of NH_2 groups
892-896	deformations of CH_2 groups for β-1,4-glycosidic bonds
~650	binding vibrations of NH_2 groups

Table 3

The inhibition of the replicating microorganism growth under the action of the COS produced by the EBP-stimulated chitosan destruction

Test microorganism	EBP-treated chitosan concentration (μg/ml)				Control
	1000	500	250	125	
E. coli	----	±	±	+	+
S. aureus	----	±	+	+	+

--- the absence of microorganism growth; ± weak microorganism growth; + microorganism growth comparable with reference sample